

⁷The Oceans Institute and School of Environmental Systems Engineering, M047 University of Western Australia, Crawley 6009 WA, Australia

Received: 14 January 2013 – Accepted: 15 January 2013 – Published: 1 March 2013

Correspondence to: A. M. Waite (anya.waite@uwa.edu.au)

Published by Copernicus Publications on behalf of the European Geosciences Union.

BGD

10, 3951–3976, 2013

Formation and maintenance of high-nitrate and low pH layers

A. M. Waite et al.

Title Page

Abstract

Introduction

Conclusions

References

Tables

Figures



Back

Close

Full Screen / Esc

Printer-friendly Version

Interactive Discussion



Abstract

We investigate the biogeochemistry of Low Dissolved Oxygen High Nitrate layers forming against the backdrop of several interleaving regional water masses in the Eastern Indian Ocean, off northwest Australia adjacent to Ningaloo Reef. These water masses, including the forming Leeuwin Current, have been shown directly to impact the ecological function of Ningaloo Reef and other iconic coastal habitats downstream. Our results indicate that LODHN layers are formed from multiple subduction events of the Eastern Gyral Current beneath the Leeuwin Current (LC); the LC originates from both the Indonesian Throughflow and tropical Indian Ocean. Density differences of up to 0.025 kg m^{-3} between the Eastern Gyral Current and the Leeuwin Current produce sharp gradients that can trap high concentrations of particles (measured as low transmission) along the density interfaces. The oxidation of the trapped particulate matter results in local depletion of dissolved oxygen and regeneration of dissolved nitrate (nitrification). We document an associated increase in total dissolved carbon dioxide, which lowers the seawater pH by 0.04 units. Based on isotopic measurements ($\delta^{15}\text{N}$ and $\delta^{18}\text{O}$) of dissolved nitrate, we determine that $\sim 40\text{--}100\%$ of the nitrate found in LODHN layers is likely to originate from nitrogen fixation, and that regionally, the importance of N fixation in contributing to LODHN layers is likely be highest at the surface and offshore.

1 Introduction

Nitrogen (N) sources entering the surface ocean via nitrogen fixation are in some cases the dominant source of bioavailable N supporting primary production (Codispoti, 2007; Gruber, 2011). This fixation of N is biologically linked to simultaneous fixation of carbon (C) into planktonic biomass, which may sink to the deep sea (Siegenthaler and Sarmiento, 1993). The relative importance upward of turbulent fluxes of N into the surface ocean across the pycnocline as new nitrate, the fluxes entering the surface ocean

BGD

10, 3951–3976, 2013

Formation and maintenance of high-nitrate and low pH layers

A. M. Waite et al.

Title Page

Abstract

Introduction

Conclusions

References

Tables

Figures

⏪

⏩

◀

▶

Back

Close

Full Screen / Esc

Printer-friendly Version

Interactive Discussion

measurements, and utilise the nitrogen and oxygen isotopic signature of dissolved nitrate ($\delta^{15}\text{N}$ and $\delta^{18}\text{O}$), to distinguish the sources of the nitrate between upward fluxes of subsurface N as new nitrate and a flux due to nitrogen fixation. We link shallow re-generation of nitrate in the LODHN layers with their impact on the carbonate system. TCO_2 generation by organic matter remineralisation causes a lowering of pH and a decrease in dissolved oxygen concentrations in the subsurface LDOHN layers.

2 Materials and methods

2.1 Primary research voyage

We sampled coastal waters from the 50 m to the 1000 m isobaths, along seven transects from 21° S to 23° S off northwest Australia. Here, the Leeuwin Current consolidates from several surface pathways, including warm and saline waters coming from the Indonesian Throughflow (Western Pacific) and the tropical Indian Ocean, fresher Indonesian waters transported by the Eastern Gyral Current (EGC) (Domingues et al., 2007), and cooler, more saline waters from the South Indian Ocean (Fig. 1a–e; see also Rossi et al., 2013). Conductivity-Temperature-Depth (CTD) measurements were made using a rosette system that carried a Wetlabs C-StarTM transmissometer, a Seabird dissolved oxygen sensor (SBE43) and a Satlantic ISUSTM sensor. Transmission was used as an indicator of particle concentration (Karageorgis et al., 2008). Chlorophyll *a* (Parsons et al., 1984), total alkalinity and total dissolved inorganic carbon measurements were made on samples from bottles fired at up to 10 depths, with 3–4 identified as being specifically within or outside the LDOHN layer. Total dissolved inorganic carbon dioxide (TCO_2) was analysed following the colometric procedure described in (Johnson et al., 1993) and (Dickson, 2007). Total alkalinity was analysed using an open cell potentiometric titration of a 100 mL sample with 0.1N HCl after Dickson et al. (2007). The accuracy and precision of the TCO_2 and total alkalinity measurements was verified as $\pm 2 \mu\text{mol kg}^{-1}$ based on analyses of certified reference seawater

BGD

10, 3951–3976, 2013

Formation and maintenance of high-nitrate and low pH layers

A. M. Waite et al.

Title Page

Abstract

Introduction

Conclusions

References

Tables

Figures

⏪

⏩

◀

▶

Back

Close

Full Screen / Esc

Printer-friendly Version

Interactive Discussion

Formation and maintenance of high-nitrate and low pH layers

A. M. Waite et al.

Title Page

Abstract

Introduction

Conclusions

References

Tables

Figures

⏪

⏩

◀

▶

Back

Close

Full Screen / Esc

Printer-friendly Version

Interactive Discussion

samples from Scripps Institute of Oceanography. pH was calculated using the Ocean Data View software, which uses an iterative Newton method, with constants following Dickson (2007). Dissolved inorganic nitrate (Nitrate and Nitrite, hereafter Nitrate) was analyzed for all depths using Quick-ChemTM methods on a flow injection LACHAT[®] instrument as per the following protocols for nitrate + nitrite (Quik-ChemTM Method 31-107-04-1-A; detection limit $\sim 0.03 \mu\text{M}$; adapted from Wood et al., 1967). For calibration of the ISUS sensor, up-cast nitrate profiles derived from in-situ ultraviolet spectrometry of the ISUS nitrate sensor were calibrated against analysed nitrate concentrations ($r^2 = 0.95$, $n = 491$). The isotopic composition of nitrate ($\delta^{15}\text{N}$ and $\delta^{18}\text{O}$) was measured by the bacterial denitrification method (Sigman et al., 2001) at the UC Davis Stable Isotope Facility, according to standard methods (García and Gordon, 1992). The term “NO” was used as a conservative water mass tracer and calculated using the formula $9\text{NO}_3 + \text{O}_2$, as each mole of consumed O_2 will roughly release 1/9th of a mole bound N as a nitrate ion (Broecker, 1974; Whitney et al., 2007).

2.2 Other related data sets

ARGO float data along 21°S , including temperature, salinity, and oxygen data collected within 50 km of that latitude, were sourced from IMOS via the ARGO website (<http://www.argo.ucsd.edu>, <http://argo.jcommops.org>).

An earlier transit through the region on the RV Southern Surveyor about one month prior to major research voyage (April 2010) was used to occupy the Sandy Bay transect ($\sim 22^\circ \text{S}$). Five 5 CTD stations from surface to 10 m above bottom, starting inshore at $\sim 30 \text{m}$ depth and continuing to the 1000 m isobaths were sampled and nutrient and chlorophyll *a* samples (total) were taken at 10 depths as described above.

3 Results

3.1 Primary research voyage

During the primary cruise in May 2010, we identified several regional water masses and currents occurring in the study region (Domingues et al., 2007; Woo and Pattiaratchi, 2008) including Subtropical Water (STW; salinity ~ 35.2) entering from the southwest, Eastern Gyral Current (EGC; salinity ~ 34.8) waters entering from the west and northwest, and Leeuwin Current/Indonesian Throughflow (LC/ITF; salinity ~ 35.6) from the north and northeast (Fig. 1a). Low dissolved oxygen high nitrate (LODHN) layers, whose overall importance had been established in our previous work (Thompson et al., 2011; Rossi et al., 2013), were visible between 100 and 250 m. These layers appeared as sharp gradients in both dissolved nitrate and oxygen with depth, associated specifically with low salinity waters (Fig. 1a–e). The profiles indicated local maxima in density gradients immediately above these layers (e.g. $\Delta\rho = 0.025$; Fig. 1a–e) above which appeared a local minimum in transparency (Fig. 1e), correlated with increased particle concentration (Karageorgis et al., 2008). The LODHN layers therefore occurred immediately below, sometimes partially overlapping, high particle loads as indicated by low transmission (Figs. 1a–e, 2a, red arrow). However, where low transmission occurred without low salinity (i.e. not adjacent to a density interface), it was not associated with a local nitrate peak (Fig. 2a, black arrow).

TCO_2 increases and O_2 minima were associated with the lowest pH values observed in surface waters (Fig. 2b). Low O_2 values were correlated with peaks in nitrate, but each peak showed a slightly different oxygen concentration (Fig. 3a). These peaks co-occur with TCO_2 maxima, such that:

$Oxygen (mol\ kg^{-1}) = -0.52 * TCO_2 (mol\ kg^{-1}) + 1237 (r = -0.80, n = 59, p < 0.0001).$

However, the anomalies did appear at many different densities between $\delta = 24$ –26, along the mixing lines between STW and EGC, and even up into the LC waters (Fig. 3b) associated with low transmission. These anomalies are regional in scale (~ 1000 km; Figs. 2c, 4).

BGD

10, 3951–3976, 2013

Formation and maintenance of high-nitrate and low pH layers

A. M. Waite et al.

Title Page

Abstract

Introduction

Conclusions

References

Tables

Figures

⏪

⏩

◀

▶

Back

Close

Full Screen / Esc

Printer-friendly Version

Interactive Discussion



Oxygen data along 21° S from the ARGO floats showed that the low oxygen layers identified in the boundary region of the eastern Indian Ocean off Western Australia continued west as far as 104° E and even to 102° E, at a similar depth range as seen in the cruise data (Fig. 5).

When we combine the O₂ and NO₃ signatures as NO and compare with potential temperature we correct for the change in gas solubility with depth (Broecker, 1974; Whitney et al., 2007) and the shallower nitrate peaks become more obvious (Fig. 6). The shallow high nitrate anomalies occur at several distinct potential temperatures: potT = 21, 23, 25 °C, all within the density range $\rho = 24\text{--}26 \text{ kg m}^{-3}$, and all at locally low salinities (~ 35). NO increases are driven locally by nitrate increases in each layer, and are particularly marked at potT = 25 °C and at 100–150 m depth. The multiple LODHN layers we identified all occurred at lower than ambient salinities ~ 35 , but at a wide range of temperatures, and densities.

Critical to a deeper understanding of the processes controlling production in the region is an understanding of the origin of these subsurface nitrate maxima consistently observed within the study area in autumn (Thompson et al., 2011; Rossi et al., 2013). The isotopic signature of the dissolved nitrate shows two groups of $\delta^{18}\text{O}$, and a clear separation between them, with $\delta^{18}\text{O}$ of surface nitrate relatively heavy ($\delta^{18}\text{O} \sim 20 \text{ ‰}$) and the $\delta^{18}\text{O}$ of deep nitrate significantly lighter ($\delta^{18}\text{O} \sim 10 \text{ ‰}$; 200–1000 m) (Fig. 7a). The $\delta^{18}\text{O}$ of nitrate decreased significantly with depth ($p < 0.001$, $R^2 = 0.46$, $n = 29$) (this trend was significant across all Groups 1, 2, and 3 below).

The $\delta^{15}\text{N}$ of deep nitrate was uniformly $\sim 6\text{--}7 \text{ ‰}$ at 200–1000 m, Fig. 7a). However, nitrate with a surface $\delta^{18}\text{O}$ signal of $\sim 20 \text{ ‰}$ contained two groupings – one with the deep nitrate signature of $\sim 6\text{--}7 \text{ ‰}$, and another small cluster of points where $\delta^{15}\text{N} = -1$ to 2 ‰, a signature of nitrogen fixation (Fig. 7a) (Montoya et al., 2002). This separated the DIN into three separate pools: Group 1: low $\delta^{15}\text{N}$ (-1 to 4 ‰) and high $\delta^{18}\text{O}$ ($\sim 22 \text{ ‰}$), Group 2: elevated $\delta^{15}\text{N}$ (7–11 ‰) and high $\delta^{18}\text{O}$ ($\sim 22 \text{ ‰}$), and Group 3: high $\delta^{15}\text{N}$ ($\sim 6.6 \text{ ‰}$) and low $\delta^{18}\text{O}$ ($\sim 10 \text{ ‰}$), and (Fig. 7a).

BGD

10, 3951–3976, 2013

Formation and maintenance of high-nitrate and low pH layers

A. M. Waite et al.

Title Page

Abstract

Introduction

Conclusions

References

Tables

Figures



Back

Close

Full Screen / Esc

Printer-friendly Version

Interactive Discussion

visible, nor were there any sub-surface salinity minima, as seen during the primary research voyage in May 2010. North of Northwest Cape, a regional bloom of the nitrogen fixing cyanophyte *Trichodesmium* was identified as distinctive pink-orange surface slicks reaching to 20° S.

4 Discussion

We suggest that spatial coupling between nitrate, transmission and oxygen across the study region indicate the presence of rapid respiration processes which consume oxygen and remineralise nutrients locally, forming low pH layers at interfaces created by the subduction of low salinity waters. Our evidence supports the production of these layers occur at small-scales (100 m in the vertical) and in the short term (weeks). We show the accumulation of organic matter at the interface of LODHN layers, as we had speculated might occur (Rossi et al., 2013). In situ local biogeochemical processes (nitrification and nitrogen fixation) are major contributors to the formation, and maintenance of the subsurface nitrate maxima, although the advection by oceanic currents of peculiar biogeochemical characteristics also play a role.

4.1 Oceanographic history and formation of LODHN layers

A transit voyage one month earlier anecdotally detected salinities at the surface which were consistent with EGC waters. These waters had low but detectable dissolved nitrate concentrations, as well as a visible bloom of the N-fixing cyanobacterium, *Trichodesmium* to the north covering 100 of square kilometers (A. Waite, unpublished data). The seasonal acceleration of warm, more saline Leeuwin Current surface water in the Austral Autumn (Domingues et al., 2007) observed in this study is therefore likely to have occurred regionally in the intervening month, subducting the lower salinity EGC layer beneath it (see schematic, Fig. 8). The deeper boundary of the low salinity layer(s) seems to then have become a “hot-spot” for remineralisation. Our analysis,

BGD

10, 3951–3976, 2013

Formation and maintenance of high-nitrate and low pH layers

A. M. Waite et al.

[Title Page](#)

[Abstract](#)

[Introduction](#)

[Conclusions](#)

[References](#)

[Tables](#)

[Figures](#)

[⏪](#)

[⏩](#)

[◀](#)

[▶](#)

[Back](#)

[Close](#)

[Full Screen / Esc](#)

[Printer-friendly Version](#)

[Interactive Discussion](#)



including the observation multiple LODHN layers with distinctive oxygen signatures, suggests further complex interleaving of water masses of different temporal origins, possibly with different oxygen histories.

The WOCE data set north of this region (e.g. IR10 http://www-pord.ucsd.edu/whp_atlas/indian/i10/prop_plots/prop_plots.htm) suggests that surface waters with salinity of $\sim 35\%$ occur in general north of 15°S for most of the year, and are a likely source for the low salinity layer we observed, including cool and variable temperatures, low dissolved oxygen and total alkalinity (2280–2300 at $20\text{--}25^\circ\text{C}$). Property plots also show low dissolved oxygen associated with high nitrate values, originating from the north as far as 10°S on the WOCE IR10 line and east into the Indonesian Throughflow (ITF) region (WOCE line IR6C). Wijffels and co-workers (Wijffels et al., 2002) suggest that the ITF carries the high-nutrient low-oxygen signal from the shallow waters off Indonesia, and that this water mass becomes more saline as it recirculates westward, before flowing eastward to form the Leeuwin Current (LC). Later work has shown that both Indian and Indonesian tropical sources are important in forming the LC, but that different recirculation times of ITF waters between Australia and Indonesia (the so-called “S” and “C” trajectories) result in markedly different T/S properties further south in the forming LC (Domingues et al., 2007). The “S” trajectories provide the freshest and warmest water source to 22°S , emerging adjacent to shore in the LC formation region, while the “C” trajectories enter the LC formation region slightly further offshore and slightly deeper (Domingues et al., 2007). The May–June autumn acceleration of the Leeuwin Current (LC) seems to favour sources from the longer “S” route (Domingues et al., 2007), and the LC waters in our study appear similarly close to the Western Australian coast, and at the surface, suggesting that the surface waters we observed are likely to have originated from the “S” route.

The Eastern Gyral Current (EGC) emerges as a key player in the formation of LODHN layers. The EGC forms from a retroflexion of the South Equatorial Current, but loses heat in the tropical-subtropical transition area before a significantly cooled and slightly more saline branch moves south towards Northwest Cape at about 22°S

BGD

10, 3951–3976, 2013

Formation and maintenance of high-nitrate and low pH layers

A. M. Waite et al.

Title Page

Abstract

Introduction

Conclusions

References

Tables

Figures

⏪

⏩

◀

▶

Back

Close

Full Screen / Esc

Printer-friendly Version

Interactive Discussion

(Domingues et al., 2007). It is these waters that are sub-ducted by, or sub-duct under, the LC waters of varying salinities that accelerate SW along the Australian northwest shelf during the Austral Autumn (May–June). Our observations near Sandy Bay, Northwest Cape (~ 22° S) about 1 month earlier in April show EGC waters from the surface to about 100 m. By May, the EGC waters were sub-ducted in a complex series of layers beneath the LC waters. We suggest that this puts a 3–4 week time line on the formation of LODHN layers, consistent with the ~ 1 month time line estimated to advect the interleaving water masses southward by 2–4 °C of latitude (Domingues et al., 2007).

4.2 Sources of particles

Remineralisation will be optimized if a sources of organic matter from the surface are available for export, accumulating at strong interfaces (Macintyre et al., 1995). We initially speculated that dense-water formation originating from the shelf during the autumn/winter period, as documented further south (Pattiaratchi et al., 2011), could play a role in contributing to particles' movement offshore (Rossi et al., 203). Our data clearly feature significant near-shore sources of particles which would theoretically drive significant oxygen depletion in LODHN layers. However, we also observed low-transparency, particle-rich layers (Karageorgis et al., 2008) at multiple locations within the mixing line between the Eastern Gyral Current waters and the more saline STW which moves shorewards from the southwest, penetrating deeper and more regionally beneath the EGC and the forming Leeuwin Current. (Waite et al., 2007b). This implies that offshore sources of particles are also likely to be important in the formation of LODHN layers. This would help explain the apparent continuity of such layers as far west as 102–104° E. Once organic-rich waters are subducted under the Leeuwin Current, particles could continue to accumulate on the resulting density interface(s), favoring continued microbial regeneration there.

BGD

10, 3951–3976, 2013

Formation and maintenance of high-nitrate and low pH layers

A. M. Waite et al.

Title Page

Abstract

Introduction

Conclusions

References

Tables

Figures

⏪

⏩

◀

▶

Back

Close

Full Screen / Esc

Printer-friendly Version

Interactive Discussion

4.3 Sources of nitrogen

Our separation of nitrogen sources into three isotopic groups based on $\delta^{15}\text{N}$ and $\delta^{18}\text{O}$ allows us to distinguish dissolved nitrate originating from nitrogen fixation (Group 1) and nitrate likely to have been assimilated and then released by grazers (Group 2). We estimate that 97 % of unassimilated nitrate (Group 1) found in surface waters of the region is likely to have originated from nitrogen fixation. This suggests that N fixation had recently been a major contributor to local production. The observation of massive bloom of *Trichodesmium* in the same area 30 days previously confirms that such sources can exist locally. At that time, the LDOHN layer was not clearly observable in this area. This again seems to set a time line of days to weeks for the formation and maintenance of the LDOHN layer. In addition, it suggests offshore, surface-ocean particle sources are also likely to be strong contributors to remineralization sources for the LDOHN layers.

Our observations indicating N-fixation as an important nitrate sources is coupled with some high isotopic values of nitrate-N (Group 2) in the immediate sub-surface (20 m) suggest simultaneous rapid assimilation via grazing, generating nitrate with a nominal trophic level of 2.4. This is remarkably similar to the effective trophic level of ~ 3 calculated for surface microheterotrophs by Waite et al. (2007), and suggests rapid recycling and remineralization is important.

4.4 The carbonate system

The pH minimum in the LDOHN layer, characterized by a peak in total DIC up to $35 \mu\text{mol kg}^{-1}$, indicates that re-mineralization has occurred for long enough to decrease pH at the density interface. How low could this pH go? Theoretically, based on the observed relationships between oxygen, carbon, and pH in this system, we might expect oxygen to become fully depleted at a TCO_2 value of $2378 \mu\text{mol kg}^{-1}$, setting a limit of $\text{pH} = 7.79 (\pm 0.04)$ in surface waters $< 200 \text{ m}$, and $\text{pH} = 7.74 (\pm 0.02)$ in waters deeper than 300 m (see two separate relationships, Fig. 3). However, we note

BGD

10, 3951–3976, 2013

Formation and maintenance of high-nitrate and low pH layers

A. M. Waite et al.

Title Page

Abstract

Introduction

Conclusions

References

Tables

Figures

⏪

⏩

◀

▶

Back

Close

Full Screen / Esc

Printer-friendly Version

Interactive Discussion

that re-mineralisation of organic matter from N-fixation could produce even greater pH decreases associated with the generation of excess protons during nitrification .(Wolf-Gladrow et al., 2007). This would suggest that regions such as this one, where nitrate may be sourced significantly from N-fixation, may be more than usually exposed to changes in ocean pH.

4.5 Regional implications

We note that in comparison to other ocean basins (Broecker, 1974), the region seems depleted in oxygen, with surface NO values as low as 175, well below those documented for the open Atlantic and Pacific (Broecker, 1974). The deeper STW contains higher NO values than the LC, EGC, and associated LODHN layers, and may contribute importantly to their oxygen budget. This, and the association of low oxygen and N-fixation derived nitrification with low pH (above), heightens the importance of understanding regional controls of the oxygen budget and their impact on ecosystem dynamics in this poorly-studied region of the Indian Ocean.

The stable layering of warm-salty water over cooler fresher water in this region forms a system in which double-diffusion might be expected to occur (Turner, 1973). There is tentative evidence of double diffusion of the diffusive-layering variety, but the implications of this on the biology and hydrography remain unclear (Kelley et al., 2003), and will need further exploration for this system.

Acknowledgements. We thank C. Domingues for helpful discussions on the interleaving water masses and D. Kelly for valuable insights into double diffusion. This study was supported by an Australian Research Council Discovery Project Grant no. DP0663670 to AMW, MR and co-workers. Ship time for both the primary voyage (V04-2010) and the earlier Transit Voyage (T01-2010) was supported by the Australian Marine National Facility. ARGO data were collected and made freely available by the International Argo Program and the national programs that contribute to it (<http://www.argo.ucsd.edu>, <http://argo.jcommops.org>). The Argo Program is part of the Global Ocean Observing System. Australian Argo data was sourced from the Integrated

BGD

10, 3951–3976, 2013

Formation and maintenance of high-nitrate and low pH layers

A. M. Waite et al.

Title Page

Abstract

Introduction

Conclusions

References

Tables

Figures

⏪

⏩

◀

▶

Back

Close

Full Screen / Esc

Printer-friendly Version

Interactive Discussion

References

- 5 Broecker, W. S.: “NO”, a conservative water-mass tracer, *Earth Planet. Sci. Lett.*, 23, 100–107, doi:10.1016/0012-821x(74)90036-3, 1974.
- Casciotti, K., Sigman, D., Hastings, M. G., Böhlke, J., and Hilkert, A.: Measurement of the oxygen isotopic composition of nitrate in seawater and freshwater using the denitrifier method, *Anal. Chem.*, 74, 4905–4912, 2002.
- 10 Codispoti, L. A.: An oceanic fixed nitrogen sink exceeding 400 Tg N a⁻¹ vs. the concept of homeostasis in the fixed-nitrogen inventory, *Biogeosciences*, 4, 233–253, doi:10.5194/bg-4-233-2007, 2007.
- Dickson, A. G.: Guide to Best Practices for Ocean CO₂ Measurements, PICES Special Publication, 3, 191 pp., 2007.
- 15 Domingues, C. M., Maltrud, M. E., Wijffels, S. E., Church, J. A., and Tomczak, M.: Simulated Lagrangian pathways between the Leeuwin Current System and the upper-ocean circulation of the southeast Indian Ocean, *Deep-Sea Research Pt. 1*, 54, 797–817, doi:10.1016/j.dsr2.2006.10.003, 2007.
- García, H. E. and Gordon, L. I.: Oxygen solubility in seawater: Better fitting equations, *Limnol. Oceanogr.*, 37, 1307–1312, 1992.
- 20 Gruber, N.: Warming up, turning sour, losing breath: ocean biogeochemistry under global change, *Philos. Trans. R. Soc. A-Math. Phys. Eng. Sci.*, 369, 1980–1996, doi:10.1098/rsta.2011.0003, 2011.
- Johnson, K. M., Wills, K. D., Butler, D. B., Johnson, W. K., and Wong, C. S.: Coulometric total carbon dioxide analysis for marine studies: maximizing the performance of an automated continuous gas extraction system and coulometric detector, *Mar. Chem.*, 44, 167–187, 1993.
- 25 Karageorgis, A. P., Gardner, W. D., Georgopoulos, D., Mishonov, A. V., Krasakopoulou, E., and Anagnostou, C.: Particle dynamics in the Eastern Mediterranean Sea: A synthesis based on light transmission, PMC, and POC archives (1991–2001), *Deep-Sea Res. Part 1*, 55, 177–202, doi:10.1016/j.dsr.2007.11.002, 2008.

Formation and maintenance of high-nitrate and low pH layers

A. M. Waite et al.

[Title Page](#)

[Abstract](#)

[Introduction](#)

[Conclusions](#)

[References](#)

[Tables](#)

[Figures](#)



[Back](#)

[Close](#)

[Full Screen / Esc](#)

[Printer-friendly Version](#)

[Interactive Discussion](#)



Formation and maintenance of high-nitrate and low pH layers

A. M. Waite et al.

[Title Page](#)

[Abstract](#)

[Introduction](#)

[Conclusions](#)

[References](#)

[Tables](#)

[Figures](#)

[⏪](#)

[⏩](#)

[◀](#)

[▶](#)

[Back](#)

[Close](#)

[Full Screen / Esc](#)

[Printer-friendly Version](#)

[Interactive Discussion](#)

Kelley, D. E., Fernando, H. J. S., Gargett, A. E., Tanny, J., and Ozsoy, E.: The diffusive regime of double-diffusive convection, *Prog. Oceanogr.*, 56, 461–481, doi:10.1016/s0079-6611(03)00026-0, 2003.

Macintyre, S., Alldredge, A. L., and Gotschalk, C. C.: Accumulation of marine snow at density discontinuities in the water column, *Limnol. Oceanogr.*, 40, 449–468, 1995.

Montoya, J. P., Carpenter, E. J., and Capone, D. G.: Nitrogen fixation and nitrogen isotope abundances in zooplankton of the oligotrophic North Atlantic, *Limnol. Oceanography*, 47, 1617–1628, 2002.

Parsons, T. R., Maita, Y., and Lalli, C. M.: *Manual of chemical and biological methods for seawater analysis*, Pergamon, 1984.

Pattiaratchi, C., Hollings, B., Woo, M., and Welhena, T.: Dense shelf water formation along the south-west Australian inner shelf, *Geophys. Res. Lett.*, 38, L10609, doi:10.1029/2011gl046816, 2011.

Rossi, V., Feng, M., Pattiaratchi, C. B., Roughan, M., and Waite, A. M.: Linking synoptic forcing and local mesoscale processes with biological dynamics off Ningaloo Reef, *J. Geophys. Res.*, accepted, 2013.

Siegenthaler, U. and Sarmiento, J. L.: Atmospheric carbon-dioxide and the ocean, *Nature*, 365, 119–125, 1993.

Sigman, D. M., Casciotti, K. L., Andreani, M., Barford, C., Galanter, M., and Bohlke, J. K.: A bacterial method for the nitrogen isotopic analysis of nitrate in seawater and freshwater, *Anal. Chem.*, 73, 4145–4153, 2001.

Sutherland, T., T. S. C., Wanninkhof, R., C., S., Feely, R. A., Chipman, D. W., Hales, B., Friederich, G., Chavez, F., Watson, A., Bakker, D. C. E., Schuster, U., Metzl, N., Yoshikawa-Inoue, H., Ishii, M., Midorikawa, H., Sabine, C., Hoppema, M., Olafsson, J., Arnarson, T. S., Tilbrook, B., Johannessen, T., Olsen, A., Bellerby, R., de Baar, H. J. W., Nojiri, Y., Wong, C. S., Delille, B., and N. R., B.: Climatological Mean and Decadal Change in Surface Ocean $p\text{CO}_2$, and Net Sea-air CO_2 Flux over the Global Ocean, *Deep-Sea Res. II*, 56, 554–577, 2009.

Thompson, P. A., Wild-Allen, K., Lourey, M., Rousseaux, C., Waite, A. M., Feng, M., and Beckley, L. E.: Nutrients in an oligotrophic boundary current: Evidence of a new role for the Leeuwin Current, *Prog. Oceanogr.*, 91, 345–359, doi:10.1016/j.pcean.2011.02.011, 2011.

Turner, J.: *Buoyancy Effects in Fluids*, Cambridge University Press, Cambridge, England, 367 pp., 1973.

Formation and maintenance of high-nitrate and low pH layers

A. M. Waite et al.

[Title Page](#)

[Abstract](#)

[Introduction](#)

[Conclusions](#)

[References](#)

[Tables](#)

[Figures](#)



[Back](#)

[Close](#)

[Full Screen / Esc](#)

[Printer-friendly Version](#)

[Interactive Discussion](#)

- Waite, A. M., Muhling, B. A., Holl, C. M., Beckley, L. E., Montoya, J. P., Strzelecki, J., Thompson, P. A., and Pesant, S.: Food web structure in two counter-rotating eddies based on delta N-15 and delta C-13 isotopic analyses, *Deep-Sea Res. Pt. 1*, 54, 1055–1075, doi:10.1016/j.dsr2.2006.12.010, 2007a.
- 5 Waite, A. M., Thompson, P. A., Pesant, S., Feng, M., Beckley, L. E., Domingues, C. M., Gaughan, D., Hanson, C. E., Holl, C. M., Koslow, T., Meuleners, M., Montoya, J. P., Moore, T., Muhling, B. A., Paterson, H., Rennie, S., Strzelecki, J., and Twomey, L.: The Leeuwin Current and its eddies: An introductory overview, *Deep-Sea Res. Pt. 1*, 54, 789–796, doi:10.1016/j.dsr2.2006.12.008, 2007b.
- 10 Whitney, F. A., Freeland, H. J., and Robert, M.: Persistently declining oxygen levels in the interior waters of the eastern subarctic Pacific, *Prog. Oceanogr.*, 75, 179–199, 2007.
- Wijffels, S., Sprintall, J., Fioux, M., and Bray, N.: The JADE and WOCE I10/IR6 Throughflow sections in the southeast Indian Ocean, Part 1: water mass distribution and variability, *Deep-Sea Res. Pt. 2*, 49, 1341–1362, doi:10.1016/s0967-0645(01)00155-2, 2002.
- 15 Wolf-Gladrow, D. A., Zeebe, R. E., Klaas, C., Koertzing, A., and Dickson, A. G.: Total alkalinity: The explicit conservative expression and its application to biogeochemical processes, *Mar. Chem.*, 106, 287–300, 2007.
- Woo, M. and Pattiaratchi, C.: Hydrography and water masses off the western Australian coast, *Deep-Sea Res. Pt. 1*, 55, 1090–1104, doi:10.1016/j.dsr.2008.05.005, 2008.
- 20 Wyatt, A. S. J., Waite, A. M., and Humphries, S.: Variability in Isotope Discrimination Factors in Coral Reef Fishes: Implications for Diet and Food Web Reconstruction, *PLoS ONE*, 5, e13682, doi:10.1371/journal.pone.0013682, 2010.

Formation and maintenance of high-nitrate and low pH layers

A. M. Waite et al.

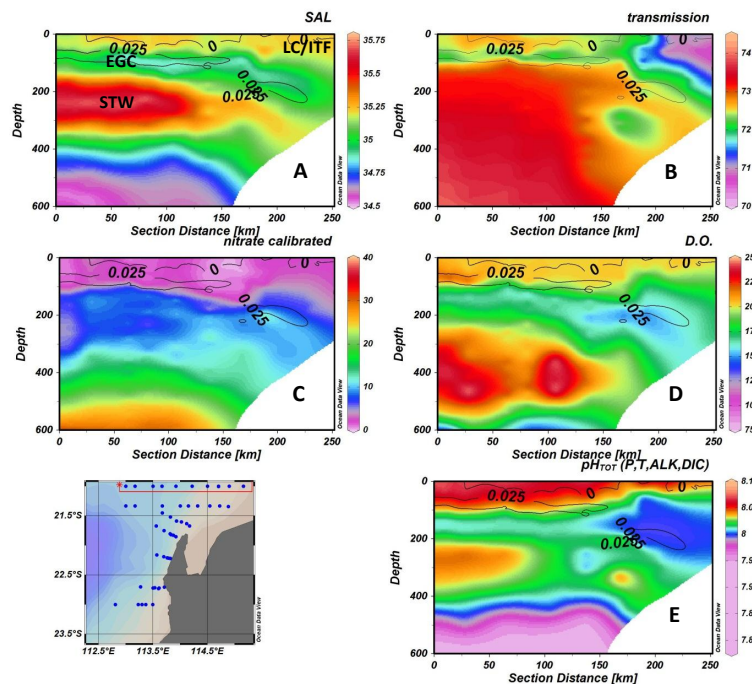


Fig. 1. Longitudinal depth profiles along 21° S transect. **(A)** salinity with major water masses (LC, Leeuwin Current; EGC, East Gyral Current; STW, Subtropical Waters), Black contour lines in all panels represent the first derivative of density with depth ($d/dz\rho$), whose maximum occurs at $\Delta\rho = 0.025$. **(B)** Transmission, as a voltage (lower values indicate higher particle concentrations); **(C)** nitrate concentrations; **(D)** dissolved Oxygen concentrations, black arrow indicating low oxygen layer, **(E)** pH, derived from total alkalinity and Dissolved Inorganic Carbon. Map indicates study area with 21° S transect highlighted in red. “SB” Denotes the Sandy Bay transect, which was occupied during the primary research voyage and also one month earlier, in April 2010.

Title Page

Abstract

Introduction

Conclusions

References

Tables

Figures



Back

Close

Full Screen / Esc

Printer-friendly Version

Interactive Discussion

BGD

10, 3951–3976, 2013

Formation and maintenance of high-nitrate and low pH layers

A. M. Waite et al.

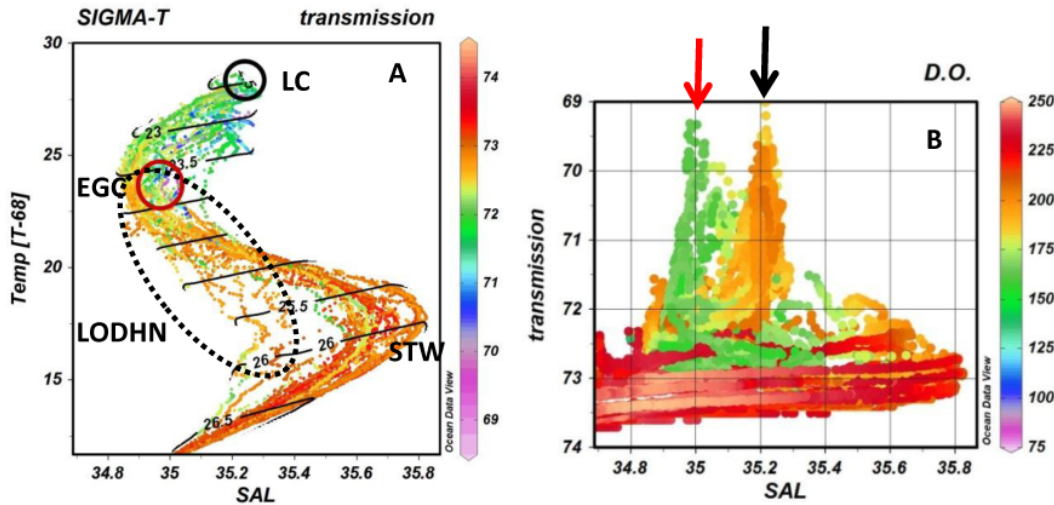


Fig. 2. Caption on next page.

Title Page

Abstract Introduction

Conclusions References

Tables Figures

⏪ ⏩

◀ ▶

Back Close

Full Screen / Esc

Printer-friendly Version

Interactive Discussion

Formation and maintenance of high-nitrate and low pH layers

A. M. Waite et al.

Fig. 2. Identifying particle rich layers: **(A)** temperature vs. salinity plot with density contours, showing high salinity subtropical water (STW) beneath tropical waters of the fresher Eastern Gyral Current (EGC) overlain with warmer, more saline Leeuwin Current waters at the surface (LC), probably sourced from the Indonesian Throughflow (ITF). Transmission is indicated as dot colour. Transmission minima (maxima of particle concentrations) are seen within the forming Leeuwin Current (LC) waters ($T = 28$, salinity = 35.3) and the Eastern Gyral Current (EGC) which is cooler and fresher ($T \sim 24$, salinity ~ 34.9). LODHN layers are visible between $\rho = 24$ and 26 show salinity profiles scattered between $\rho = 24$ and 26.5 (dashed oval). **(B)** Relationship between transmission and salinity with dissolved oxygen ($\mu\text{mol kg}^{-1}$) as dot colour. Note that the two transmission minima, at salinity = ~ 35 and salinity = ~ 35.2 ; just offset from the LC and EGC water properties. The maximum at salinity = 35 is a major LODHN layer whose intrusion creates the $\Delta\rho = 0.025$ anomaly (Fig. 1) (indicated with red arrow; see also red circle on Fig. 3), with nitrate concentrations $\sim 2\text{--}10 \mu\text{mol L}^{-1}$. Black arrow indicates more saline, warmer waters of the Leeuwin Current, in which nitrate has not been generated despite high transmission; oxygen remains high (see black circle, Fig. 3). Both peaks have relatively low NO properties, but in the fresher peak has a much higher nitrate: oxygen ratio (see also Fig. 5).

Title Page

Abstract

Introduction

Conclusions

References

Tables

Figures

⏪

⏩

◀

▶

Back

Close

Full Screen / Esc

Printer-friendly Version

Interactive Discussion

Formation and maintenance of high-nitrate and low pH layers

A. M. Waite et al.

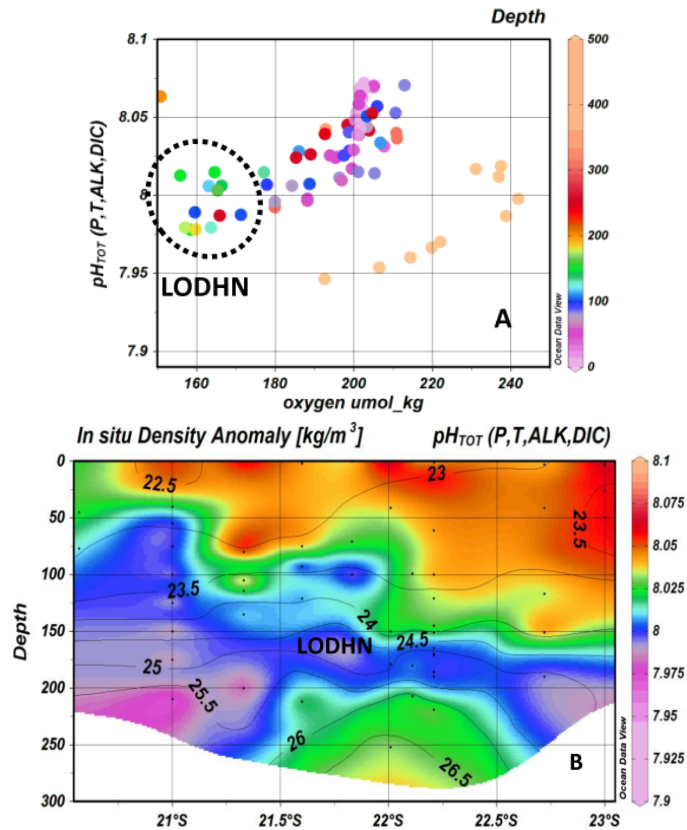


Fig. 3. (A) pH declines with lower oxygen concentrations in waters shallower than 200 m, such that pH minima occur where oxygen concentrations are $< 160 \mu\text{mol kg}^{-1}$. Note that there are two separate relationships between oxygen and pH, one shallower than 200 m and one below 400 m depth. (B) Meridional pH anomaly along the ~ 200 m contour (roughly $114\text{--}113.5^\circ\text{E}$) across the study region.

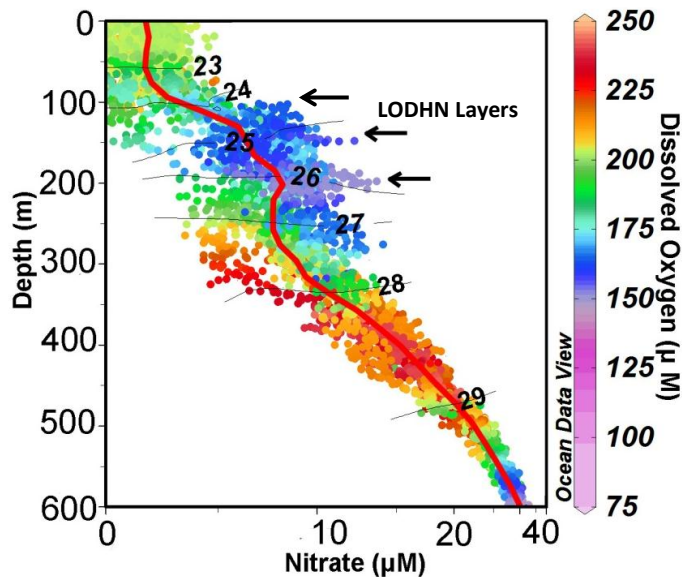


Fig. 4. (1) Depth profile plot of nitrate concentrations with dissolved oxygen concentrations overlay and in situ density contour lines in black, from 21° S transect. Several LDOHN layers are visible just below the $\rho = 24$ density isoline, and between $\rho = 25$ – 26 isolines (Black arrows) and below $\rho = 27$. Note that oxygen is locally lowered below saturation in each LODHN layer, but each layer has a different characteristic oxygen signal (seen as varying pale blue, dark blue and purple shading of dots) Data from transect 1 (Fig. 1f) was fitted through piece-wise linear least squares function. (2) Temperature vs. salinity plot with density contours, showing high salinity subtropical water (STW) beneath tropical waters of the fresher Eastern Gyral Current (EGC) overlain with warmer, more saline Leeuwin Current waters at the surface (LC). Transmission is indicated as dot colour, with coloured circles indicating high transmission peaks identified in Fig. 2. LODHN layers are visible between $\rho = 24$ and 26 slow salinity profiles scattered between $\rho = 24$ and 26.5 (dashed oval).

Formation and maintenance of high-nitrate and low pH layers

A. M. Waite et al.

Title Page	
Abstract	Introduction
Conclusions	References
Tables	Figures
◀	▶
◀	▶
Back	Close
Full Screen / Esc	
Printer-friendly Version	
Interactive Discussion	



Formation and maintenance of high-nitrate and low pH layers

A. M. Waite et al.

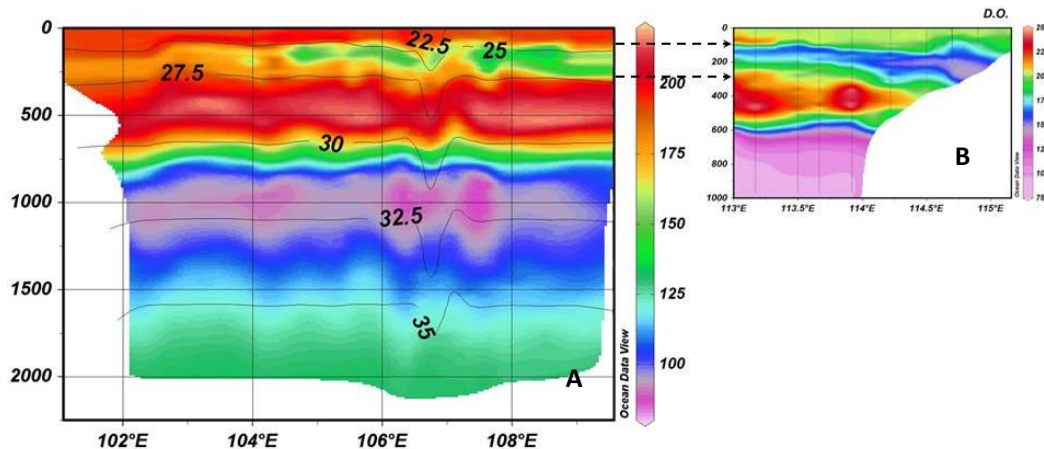


Fig. 5. Dissolved oxygen concentrations in $\mu\text{mol kg}^{-1}$ along 21° S. **(A)** Compilation of all available regional oxygen data from profiling Argo floats, showing that the oxygen minimum is regional in scale, centred just above 200 m. **(B)** Primary research cruise data from 21° S (adapted from Fig. 1d) match, spatially, reasonably well with the Argo data despite very different spatial and temporal scales.

Title Page

Abstract

Introduction

Conclusions

References

Tables

Figures

⏪

⏩

◀

▶

Back

Close

Full Screen / Esc

Printer-friendly Version

Interactive Discussion

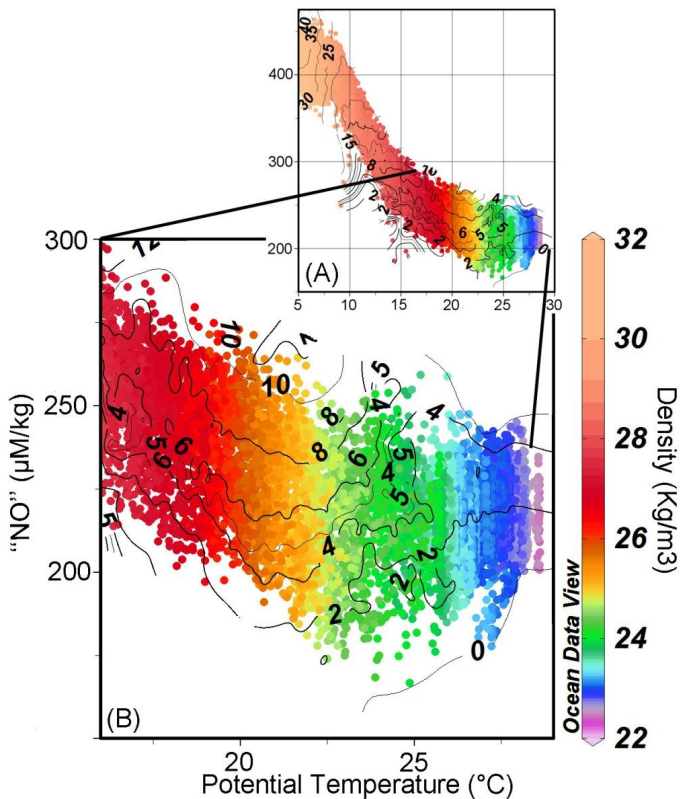


Fig. 6. Plot of “NO” versus potential temperature with in situ density overlay and nitrate concentration contour lines in black from all the data collected in the study area. LDOHN layer at $\rho = 24$ density isoline, with peaks at $\rho = 25$ – 26 isoline. Sharp increase in nitrate concentrations from ~ 2 to 5 – $10 \mu\text{mol L}^{-1}$ within 10 – 20 m.

Formation and maintenance of high-nitrate and low pH layers

A. M. Waite et al.

Title Page

Abstract Introduction

Conclusions References

Tables Figures

⏪ ⏩

◀ ▶

Back Close

Full Screen / Esc

Printer-friendly Version

Interactive Discussion



Formation and maintenance of high-nitrate and low pH layers

A. M. Waite et al.

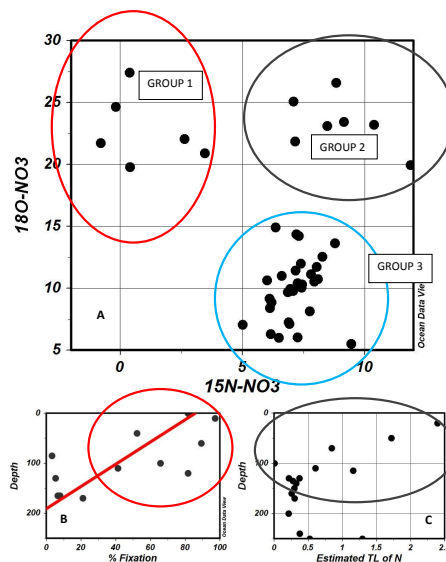


Fig. 7. (A) Isotopic composition of dissolved nitrate across the study region. A $\delta^{15}\text{N}$ near zero is classically evidence of nitrogen fixation as an N source, while deep nitrate classically has a regional signature of $\sim 6.6\text{‰}$. Near-surface $\delta^{18}\text{O}$ sources are known to be enriched in $\delta^{18}\text{O}$ due to preferential evaporation of ^{16}O over ^{18}O . GROUP 1: nitrate produced using fixed nitrogen and surface oxygen (Red circle) GROUP 2: nitrate produced using surface oxygen and nitrogen from non-fixation sources, likely to be grazing (Montoya et al., 2002) (black circle). Nitrate produced at depth conforming to the regional mean of $\delta^{15}\text{N} = 6.6\text{‰}$ (Waite et al., 2007) (Blue Circle). (B) Derived value for % of nitrate originating from nitrogen fixation based on a simple linear isotope mixing model, with a fixation end point $\delta^{15}\text{N} = -1\text{‰}$, and deep regenerated nitrate $\delta^{15}\text{N} = 6.6\text{‰}$. (C) Speculative estimation of the source trophic level (TL) of regeneration for the measured nitrate – based on the $\Delta\delta^{15}\text{N}$ of 2.2 per trophic level we estimated for the oligotrophic Indian Ocean by (Waite et al., 2007a; see text for details).

Title Page

Abstract

Introduction

Conclusions

References

Tables

Figures

◀

▶

◀

▶

Back

Close

Full Screen / Esc

Printer-friendly Version

Interactive Discussion

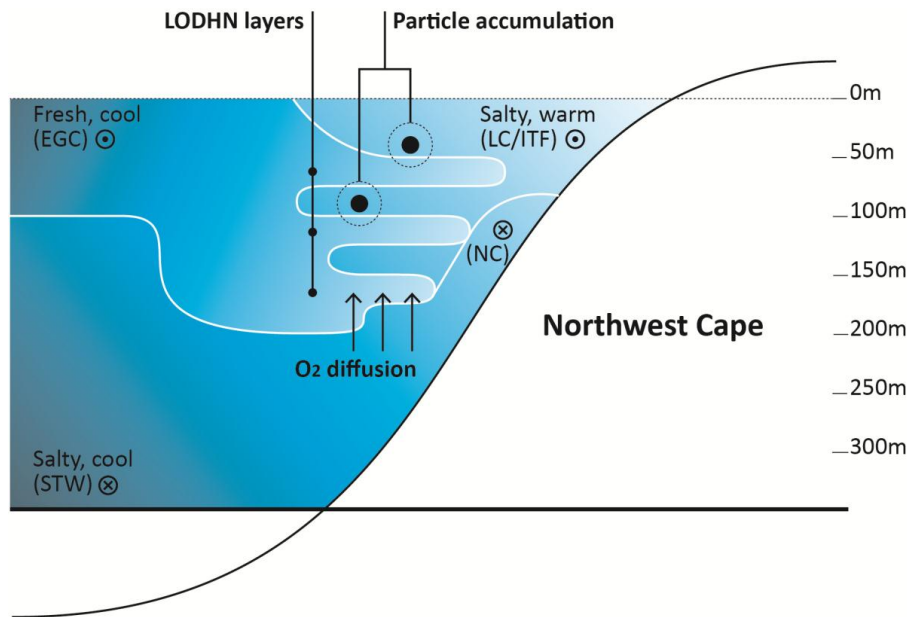


Fig. 8. Schematic of formation of LODHN layers in the autumn off Northwest Cape, Western Australia. The fresh, cool water from the northwest (e.g. the Eastern Gyral Current, EGC) interleaves with arrival events of the more salty, warmer Leeuwin Current (LC) source waters from the Indonesian Throughflow (ITF) in the late summer and autumn. Periodically, the Ningaloo Current (NC) is formed near the coast due to strong southwesterly winds. The LODHN layers, containing locally high nitrate and high dissolved organic carbon, as well as low oxygen and low pH, form beneath particle-rich layers sourced variously from surface waters and dependent on local surface production for supply of particles. Nitrogen fixation accounts for a measurable fraction of the nitrate generated in LODHN waters, but is rapidly remineralized, likely by microheterotrophs.

Title Page	
Abstract	Introduction
Conclusions	References
Tables	Figures
⏪	⏩
◀	▶
Back	Close
Full Screen / Esc	
Printer-friendly Version	
Interactive Discussion	